PHYSICAL REVIEW D **86,** 055010 (2012)

Bounds on *R*-parity violation from resonant slepton production at the LHC

H. K. Dreiner* and T. Stefaniak†

Bethe Center for Theoretical Physics and Physikalisches Institut, Universität Bonn, Bonn, Germany

(Received 1 March 2012; published 11 September 2012)

We consider the ATLAS and CMS searches for dijet resonances, as well as the ATLAS search for like-sign dimuon pairs at the LHC with 7 TeV center-of-mass energy. We interpret their exclusions in terms of bounds on the supersymmetric *R*-parity–violating parameter space. For this we focus on resonant slepton production followed by the corresponding decay.

DOI: 10.1103/PhysRevD.86.055010 PACS numbers: 12.60.Jv

I. INTRODUCTION

After initial problems [1], the LHC has been running very well since November 2009. One of the main physics objectives is to search for new physics beyond the standard model of particle physics (SM), in particular also supersymmetry (SUSY) [2]. The CMS and ATLAS experiments have so far mainly concentrated on *R*-parity–conserving supersymmetry searches [3], where the lightest supersymmetric particle (LSP) is stable as well as electrically and color neutral. The corresponding searches thus employ strict cuts on the missing transverse energy, $\not{E}_T$ [4,5]. To date, no disagreement with the SM has been found, resulting in strict lower mass bounds on the new supersymmetric particles in the simplest supersymmetric models; see also [6].

R-parity violation is theoretically equally well motivated [7–11] to the *R*-parity–conserving case. It has the same particle content and the same number of imposed symmetries. In particular it automatically includes light neutrinos [12–14], without adding a new seesaw energy scale or right-handed neutrinos [15,16]. If *R* parity is replaced by baryon triality [9,17–19], the superpotential must be extended by

$$W_{B_3} = \lambda_{ijk} L_i L_j \bar{E}_k + \lambda'_{ijk} L_i Q_j \bar{D}_k + \kappa_i L_i H_u, \quad (1)$$

where we have used the notation as in [8]. These operators all violate lepton number. At a hadron collider the terms $\lambda'_{ijk} L_i Q_j \bar{D}_k$ can lead to resonant slepton and sneutrino production [20]

$$\bar{d}_j + d_k \to \tilde{\nu}_{Li}, \quad (2)$$

$$\bar{u}_j + d_k \to \tilde{\ell}^-_{Li}, \quad (3)$$

as well as the charge conjugate processes. This is our focus here, as opposed to squark and gluino pair production. The sleptons can decay via *R*-parity–violating operators:

$$\tilde{\nu}_i \to \begin{cases} \ell^+_j \ell^-_k, & L_i L_j \bar{E}_k, \quad \text{(a)} \\ d_j \bar{d}_k, & L_i Q_j \bar{D}_k, \quad \text{(b)} \end{cases} \quad (4)$$

$$\tilde{\ell}^-_i \to \begin{cases} \bar{\nu}_j \ell^-_k, & L_i L_j \bar{E}_k, \quad \text{(a)} \\ \bar{u}_j d_k, & L_i Q_j \bar{D}_k. \quad \text{(b)} \end{cases} \quad (5)$$

The sleptons can also decay to neutralinos and charginos:

$$\tilde{\nu}_i \to \begin{cases} \nu_i \chi^0_j, & \text{(a)} \\ \ell^-_i \chi^+_j, & \text{(b)} \end{cases} \quad (6)$$

$$\tilde{\ell}^-_i \to \begin{cases} \ell^-_i \chi^0_j, & \text{(a)} \\ \nu_i \chi^-_j. & \text{(b)} \end{cases} \quad (7)$$

It is the purpose of this paper to investigate resonant slepton production at the LHC via an operator $LQ\bar{D}$. We first consider the decays via the same operator, resulting in resonant dijet production. We go beyond previous work by comparing with the ATLAS [21] and CMS [22] data, and thus setting relevant bounds on the underlying *R*-parity–violating supersymmetric model.

We then consider the decay of the slepton to a neutralino. As we show below, this can lead to like-sign dileptons in the final state, due to the Majorana nature of the neutralinos. We then focus on the case of muons and compare to the ATLAS like-sign dimuon search [23].

The phenomenology of resonant slepton production was first studied in [20,24,25]. A detailed discussion focusing on the supersymmetric gauge decays resulting in a like-sign dilepton signature was presented in [26–29]. Specific benchmark points were investigated in [30]. A trilepton signature via the chargino mode in Eq. (6) was discussed in [31,32]. Since then, various aspects have been investigated. Single (squark and) slepton production leading to single top quark production was discussed in [33,34]. Resonant slepton production with a fourth family was discussed in [35], with an ultralight gravitino in [36]. All but the latter assumed a neutralino LSP. Resonant slepton production was also considered in the context of a $\tilde{\tau}$-LSP in Ref. [37]. Resonant squark and slepton production were suggested as an explanation of the CDF Wjj anomaly in Ref. [38].

Resonant slepton production has been directly searched for at the Tevatron by the D0 [39–41] and CDF experiments [42–45], setting bounds on the relevant parameters. D0 [39,40] focused on the resonant production and decay of smuons ($\tilde{\mu}$) and muon-sneutrinos ($\tilde{\nu}_\mu$) via λ'_{211}. The

*dreiner@th.physik.uni-bonn.de
†tim@th.physik.uni-bonn.de

results were presented as upper limits on λ'_{211} in the $(\tilde{\chi}^0_1, \tilde{\mu})$ mass plane within the minimal supergravity/constrained minimal supersymmetric standard model (CMSSM) [46–49] framework. The limits are roughly $\lambda'_{211} < 0.04(0.2)$ for smuon masses $m_{\tilde{\mu}} \lesssim 200$–$300(550)$ GeV. As we will see, our study of the LHC data greatly improves these limits.

CDF [50] and D0 [51] also searched for R-parity violation, assuming the (R-parity–conserving) pair production of neutralinos and/or charginos. Furthermore, CDF investigated R-parity violation in stop pair production [52]. Implications on R-parity–violating models from R-parity–conserving SUSY searches at the Tevatron have been studied in [53–55].

The $LQ\bar{D}$ operator could also lead to resonant squark production at HERA [56]. This has been searched for by both H1 [57] and ZEUS [58]. They obtain limits in terms of a squark mass. For example, for a R-parity–violating coupling of electromagnetic strength, $\lambda'_{11k} = 0.3 (k \in \{1, 2\})$, the mass bound on the corresponding right-handed down-type squark is $m_{\tilde{d}_k} \gtrsim 280$ GeV [57].

There are also a few dedicated searches for R-parity violation at the LHC. The ATLAS Collaboration has searched for resonant tau sneutrino ($\tilde{\nu}_\tau$) production followed by the R-parity–violating decay to an $e\mu$ final state; cf. Eq. (4)(a) [59]. Furthermore, a search for displaced vertices arising from R-parity–violating decays of a long-lived neutralino has been performed by ATLAS [60]. The CMS Collaboration has considered hadronic supersymmetric pair production followed by cascade decays to a neutralino. The neutralino then decays to a purely leptonic final state [61,62]. The ATLAS Collaboration has furthermore interpreted a generic search in terms of bounds on a bilinear R-parity–violating model [63]. These are models where $\lambda_{ijk}, \lambda'_{ijk} = 0$ and $\kappa_i \neq 0$; cf. Eq. (1). In general, at any given energy scale, κ_i can be rotated to zero [12,64], and we prefer to work in this basis.

The combined mass limits from LEP, assuming the R-parity–violating decay of pair-produced gauginos or sleptons via $LQ\bar{D}$ couplings, are $m_{\tilde{\chi}^0_1} \geq 39$ GeV, $m_{\tilde{\chi}^\pm_1} \geq 103$ GeV, $m_{\tilde{\nu}_{\mu,\tau}} \geq 78$ GeV and $m_{\tilde{\mu}} \geq 90$ GeV [65,66]. Note, however, that the gaugino mass limits are formally only valid in the supersymmetric parameter region investigated by LEP, i.e. for a ratio of the Higgs vacuum expectation values of $1 \leq \tan\beta \leq 35$, a universal soft-breaking scalar mass parameter $m_0 \leq 500$ GeV, a Higgs mixing parameter $|\mu| \leq 200$ GeV, a $SU(2)$ gaugino mass parameter $M_2 \leq 500$ GeV and an R-parity–violating coupling larger than 10^{-4}.

Upper bounds on single $LQ\bar{D}$ couplings from flavor physics and/or from atomic parity violation have been derived and summarized in [7,66–69]. These bounds usually scale with the up- or down-type squark mass and thus basically do not constrain R-parity–violating effects in the case where the squarks are decoupled from the low energy spectrum, which is the case in our analyses.

II. RESONANT SLEPTONS AT THE LHC

A. Production process

We consider the single production of a slepton at the LHC [Eqs. (2) and (3)]. Note that only the $SU(2)$ doublet left-handed component of the slepton field couples to this operator. We assume the singly produced slepton to be purely left-handed. We therefore omit the subscript L in the following. The case of non-negligible mixing of the weak eigenstates—as usually relevant for the third-generation slepton, the stau—will be briefly discussed below.

For resonant production, the next-to-leading order (NLO) calculations, including QCD and supersymmetric QCD corrections, have been performed in Refs. [30,70–72]. They increase the LO cross section at the 14 TeV LHC by a K factor of up to 1.35 for slepton masses less then 2 TeV, while reducing the uncertainty from the renormalization and factorization scale dependence[1] to less than 5% [30]. Further, the authors of Ref. [30] have shown that the dependence on the parton density function (PDF) parametrization is less than 5% by comparing the cross sections obtained by the CTEQ6M [73] and the MRST04 [74,75] fits. We do not expect these uncertainties to change dramatically for the LHC at a center-of-mass energy of $\sqrt{s} = 7$ TeV and therefore adopt these numbers for this study.

The single slepton ($\tilde{\nu}^{(*)} + \tilde{\ell}^\pm$) production cross section at the 7 TeV LHC, including NLO QCD corrections (as employed here), is shown in Fig. 1, as a function of the joint slepton mass, $\tilde{m}$. We used the CTEQ6M [73] PDFs and set the renormalization and factorization scale equal to the slepton mass, $\mu_R = \mu_F = \tilde{m}$. The red bands in Fig. 1 indicate the total theoretical uncertainty of 7%, including both scale uncertainties and PDF parametrization, which are added in quadrature.

In Fig. 1 we present the cross sections $\sigma(\lambda', \tilde{m})$ for the R-parity–violating couplings $\lambda'_{ijk} = 0.01$ which couple to the first- and second-generation quarks ($j, k \in \{1, 2\}$). The highest cross section is obtained for λ'_{i11} since it involves valence quarks in all cases. The rate for second-generation quarks is suppressed, due to the lower parton luminosity of the sea quarks. $\sigma(\lambda'_{i12})$ is slightly larger than $\sigma(\lambda'_{i21})$ due to the large u quark flux.

Exemplary event rates are shown in Table I for 1 fb^{-1} of LHC data at 7 TeV. Here $\lambda' = 0.01$; the cross section scales with $(\lambda')^2$. We further list the number of singly produced $\tilde{\ell}^+$, $\tilde{\ell}^-$ and $\tilde{\nu} + \tilde{\nu}^*$ separately. For instance, for a slepton mass $\tilde{m} = 500$ GeV and an R-parity–violating coupling $\lambda'_{i11} = 0.01(0.005)$, we expect in total 80.8(20.2) signal events, of which the production of a charged slepton comprises 58%. The $\tilde{\ell}^+$ rate differs from the $\tilde{\ell}^-$ rate, since they

[1]We checked this by varying the factorization scale, μ_F, and renormalization scale, μ_R, over the range $\tilde{m}/2 \leq \mu_F, \mu_R \leq 2\tilde{m}$ for the 7 TeV cross section estimate. The deviations from the value obtained at $\mu_R = \mu_F = \tilde{m}$ are less than 3%.

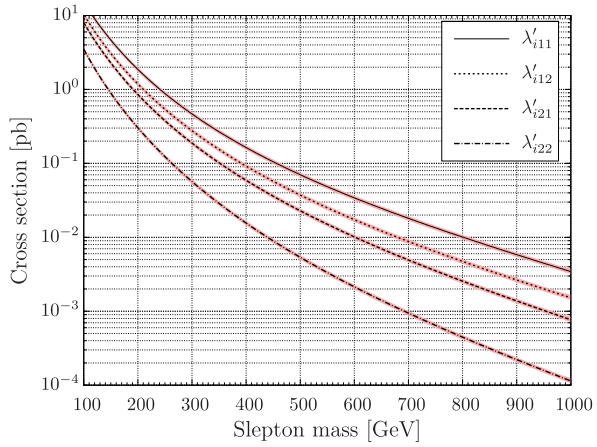

FIG. 1 (color online). Single slepton production cross section including QCD NLO corrections at the LHC for $\sqrt{s} = 7$ TeV as a function of the slepton mass, $m_{\tilde{\ell}}$, for $(\lambda'_{i11}, \lambda'_{i12}, \lambda'_{i21}, \lambda'_{i22}) = 0.01$. The CTEQ6M PDFs have been used, and renormalization and factorization scales have been identified with the slepton mass $m_{\tilde{\ell}}$. The red bands correspond to an estimated 7% systematic uncertainty, including PDF and renormalization/factorization scale uncertainties.

involve different parton fluxes. In the case of single stau production, where the right-handed component of the lightest stau, $\tilde{\tau}_1$, cannot be neglected, the cross section is suppressed by $\cos^2\theta_{\tilde{\tau}}$, where $\theta_{\tilde{\tau}}$ is the stau mixing angle.

Although SUSY-QCD corrections can be large in specific regions of the supersymmetric parameter space [30], we do not include them in order to stay as model-independent as possible. Next-to-NLO QCD corrections [76] increase the LHC cross section by 3.4%–4% compared to the NLO result. We do not include the gluon-gluon fusion production process for sneutrinos, which is only relevant for λ'_{i33} [72].

TABLE I. Number of single slepton events for an integrated luminosity of 1 fb^{-1} at $\sqrt{s} = 7$ TeV using the QCD NLO cross section. The first column shows the relevant $L_iQ_j\bar{D}_k$ coupling. The second column gives the slepton mass, $\tilde{m}$. The third, fourth and fifth columns contain the number of $\tilde{\ell}^+$, $\tilde{\ell}^-$ and $\tilde{\nu} + \tilde{\nu}^*$ events. The last column shows the sum.

λ'_{ijk}	$\tilde{m}$ [GeV]	$\tilde{\ell}^+$	$\tilde{\ell}^-$	$\tilde{\nu} + \tilde{\nu}^*$	Total
	250	365	194	428	987
$\lambda'_{i11} = 0.01$	500	32.6	14.4	33.8	80.8
	800	4.9	1.8	4.5	11.2
	250	275	47.8	309	632
$\lambda'_{i12} = 0.01$	500	21.8	2.3	21.7	45.8
	800	2.9	0.2	2.6	5.7
	250	40.2	122	211	373
$\lambda'_{i21} = 0.01$	500	1.8	7.6	13.7	23.1
	800	0.1	0.8	1.6	2.5
	250	25.0	25.0	71.5	122
$\lambda'_{i22} = 0.01$	500	1.1	1.1	3.3	5.5
	800	0.06	0.06	0.3	0.42

B. Slepton decay and signatures

We consider three possible decays of the sleptons. We first analyze the R-parity–violating decay to two jets via the production operator; cf. Eqs. (4)(b) and (5)(b). The signature is a narrow dijet resonance. We then consider the decay via a neutralino or a chargino; cf. Eqs. (6) and (7). This can lead to a like-sign dilepton final state signature. For both analyses, we shall compare our results directly with the relevant ATLAS [21,23] and CMS [22] data.

Since we cannot perform a detailed analysis while scanning over the entire supersymmetric parameter space, we restrict ourselves to three specific (simplified) lightest neutralino scenarios:

[S1] bino-like $\tilde{\chi}^0_1$.—The wino mass M_2 and the Higgs mixing parameter μ are much larger than the bino and the slepton mass (M_2, $\mu \gg M_1$, $\tilde{m}$). $\tilde{\chi}^0_1$ therefore has a large bino component. The masses of $\tilde{\chi}^0_{2,3,4}$, and $\tilde{\chi}^\pm_{1,2}$, are much larger than $m_{\tilde{\chi}^0_1}$, and $\tilde{m}$.

[S2] wino-like $\tilde{\chi}^0_1$: M_1, $\mu \gg M_2$, $\tilde{m}$.—Here, $\tilde{\chi}^0_1$ has a large wino component, and it is nearly mass degenerate with the (wino-like) $\tilde{\chi}^\pm_1$. $\tilde{\chi}^0_{2,3,4}$ and $\tilde{\chi}^\pm_2$ are again decoupled from the relevant mass spectrum.

[S3] Higgsino-like $\tilde{\chi}^0_1$: $M_1, M_2 \gg \mu, \tilde{m}$.—Here, $\tilde{\chi}^0_{1,2}$ and $\tilde{\chi}^\pm_1$ are nearly mass degenerate and have a large Higgsino component. Hence, gauge interactions of these sparticles are suppressed. The heavier neutralinos, $\tilde{\chi}^0_{3,4}$, and the heavy chargino, $\tilde{\chi}^\pm_2$, are decoupled from the relevant mass spectrum.

Note that all model parameters in this study are defined at the weak scale.

Within the framework of the CMSSM, the lightest neutralino is typically dominated by its bino component. Thus, our first simplified scenario $S1$ can be seen as a good approximation to wide regions of the CMSSM, where the resonantly produced slepton is lighter than the wino-like $\tilde{\chi}^0_2$ and $\tilde{\chi}^\pm_1$. In contrast, in anomaly-mediated SUSY breaking scenarios [77–80], the lightest neutralino is rather wino-like. For these scenarios our simplified model $S2$ can be considered an approximation. Note that this discussion neglects the influence of the Higgs mixing parameter μ. In the case of a very small value of μ the $\tilde{\chi}^0_1$ becomes Higgsino-like and thus the scenario takes on the properties of our simplified model $S3$. See also [81].

The resonant dijet processes via the operator λ'_{ijk} [Eqs. (2) and (3)] and the decays [Eqs. (4) and (5)] are depicted in Fig. 2. At tree level, the decay width is $\Gamma(\tilde{\ell}^-_i \to \bar{u}_j d_k) \approx 75$ MeV, for $\tilde{m} = 500$ GeV and $\lambda' = 0.05$ [28]. At hadron colliders, this process leads to a very narrow resonance in the invariant mass spectrum of the dijet system. However, due to the large QCD background at the LHC, it will only be visible for large slepton masses $\tilde{m} \gtrsim 1$ TeV and reasonably large R-parity–violating couplings $\lambda' \gtrsim \mathcal{O}(10^{-2})$.

If the slepton or sneutrino is the LSP, the dijet channel is the only kinematically allowed decay mode. For a $\tilde{\chi}^0_1$ LSP,

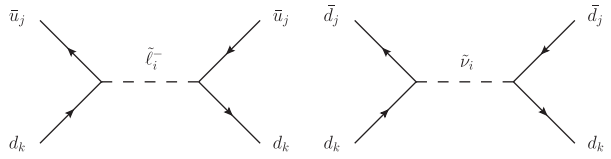

FIG. 2. Resonant production of a charged slepton, $\tilde{\ell}_i^-$, (left) and a sneutrino, $\tilde{\nu}_i$, (right), followed by the direct decay into two quarks via the R-parity–violating coupling λ'_{ijk}. This process leads to a narrow dijet resonance.

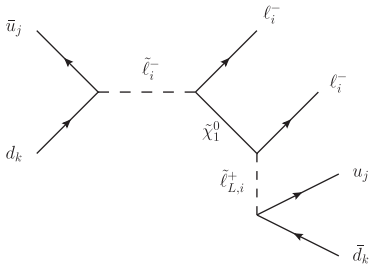

FIG. 3. Resonant production of a charged slepton, $\tilde{\ell}_i$, with successive decay into the lightest neutralino, $\tilde{\chi}_1^0$, and a charged lepton, ℓ_i. The subsequent decay of the $\tilde{\chi}_1^0$ can lead to another lepton of the same charge due to the Majorana nature of the neutralino. Thus, this process gives rise to a like-sign dilepton signature.

the slepton decay to dijets is competing with the R-parity–conserving decay $(\tilde{\ell}/\tilde{\nu}) \to (\ell/\nu) + \tilde{\chi}_1^0$ and possibly other decays to lighter sparticles; cf. Eqs. (6) and (7). A typical value for the kinematically unsuppressed $(m_{\tilde{\chi}_1^0} \ll \tilde{m})$ decay width is $\Gamma(\tilde{\ell} \to \ell \tilde{\chi}_i^0) \approx 1$ GeV, for $\tilde{m} = 500$ GeV [82,83]. This broadens the dijet resonance and reduces the dijet branching ratio. The exact branching ratios depend on the R-parity–violating coupling strength λ', the composition of the light gauginos and the details of the mass spectrum. The gauge decays are basically absent in $S3$ for the first- and second-generation sleptons, but can be relevant for a scalar tau.

If χ_1^0 is the LSP, it decays via the operator $L_i Q_j \bar{D}_k$ as

$$\chi_1^0 \to \begin{cases} \ell_i^- u_j \bar{d}_k \\ \nu_i d_j \bar{d}_k \end{cases} + \text{c.c.} \tag{8}$$

The complex conjugate decays are equally likely, due to the Majorana nature of the neutralino. The neutrino and charged lepton decay modes can have different branching ratios depending on the admixture of the lightest neutralino. The decay $\chi_1^0 \to \nu_i \gamma$ for $L_i Q_j \bar{D}_k$ is only possible for $j = k$ [12] but is typically highly suppressed and not relevant for collider signatures [84].

Within the framework of the three decoupled scenarios $S1$-$S3$, only the process

$$\bar{u}_j d_k \to \tilde{\ell}^- \to \ell^- \tilde{\chi}_1^0 \xrightarrow{\lambda'} \ell^- u_j \bar{d}_k \tag{9}$$

(and its charged conjugate) can lead to a like-sign dilepton signature. One diagram contributing to this process is also illustrated in Fig. 3. The sneutrino production

$$d_j \bar{d}_k \to \tilde{\nu}^* \to \ell^+ \tilde{\chi}_1^- \tag{10}$$

followed by the decay of the chargino $\tilde{\chi}_1^- \to \ell_i^- \bar{d}_j d_k$ (via $L_i Q_j \bar{D}_k$) leads to an opposite-sign dilepton signature. The cascade decay of the chargino via the neutralino

$$d_j \bar{d}_k \to \tilde{\nu}^* \to \ell^+ \tilde{\chi}_1^- \to W^- \tilde{\chi}_1^0 \xrightarrow{\lambda'} \ell^+ \bar{u}_j d_k \tag{11}$$

in the wino-like scenario is kinematically suppressed since $\tilde{\chi}_1^-$ and $\tilde{\chi}_1^0$ are nearly mass degenerate.

In $S3$, $\tilde{\chi}_1^0$ can be replaced by $\tilde{\chi}_2^0$ in Eq. (9). The $\tilde{\chi}_1^0$ and $\tilde{\chi}_2^0$ have similar couplings due to their large Higgsino components and are again nearly mass degenerate. Thus, this process contributes with a similar rate to the like-sign dilepton signature as the process in Eq. (9). In addition, the rate is enhanced by roughly a factor of 2 compared to the bino- and wino-like $\tilde{\chi}_1^0$ scenarios because the neutral decay $\tilde{\chi}_{1,2}^0 \to \nu_i d_j \bar{d}_k$ in Eq. (8) is suppressed for a Higgsino $\tilde{\chi}_{1,2}^0$.

In Figs. 4 and 5, we show the dependence of the charged slepton branching ratios corresponding to the decays [Eqs. (5)(b) and (7)] on the lightest neutralino mass, $m_{\tilde{\chi}_1^0}$, and coupling strength, λ', respectively. In both figures we chose a slepton mass of $\tilde{m} = 500$ GeV. In Fig. 4, the R-parity–violating coupling strength is set to $\lambda' = 0.05$. In Fig. 5, we fixed the lightest neutralino mass to 250 GeV.

As $m_{\tilde{\chi}_1^0}$ increases,[2] the phase space in the gauge decays of the slepton [Eq. (7)] decreases and leads to a suppression of the R-parity–conserving decays [Eq. (5)(b)]. For $m_{\tilde{\chi}_1^0} \geq 500$ GeV, the slepton becomes the LSP and only the dijet decay channel remains accessible. Note that there are extensive regions in R-parity–violating CMSSM parameter space where the slepton is indeed the LSP [37,55,85–87].

For the bino- and wino-like $\tilde{\chi}_1^0$ scenarios (the left and middle panels in Figs. 4 and 5, respectively), we show the branching ratios $\mathcal{B}(\tilde{\ell}^+ \to u\bar{d})$, $\mathcal{B}(\tilde{\ell} \to \ell \tilde{\chi}_1^0)$ and $\mathcal{B}(\tilde{\ell}^+ \to \bar{\nu} \tilde{\chi}_1^+)$, where the charged slepton is the left-handed slepton of any of the three generations, $\tilde{\ell} = \tilde{e}_L, \tilde{\mu}_L, \tilde{\tau}_L$.

In $S1$, the only kinematically allowed slepton decays are $\tilde{\ell}^+ \to u\bar{d}$ and $\tilde{\ell} \to \ell \tilde{\chi}_1^0$. Recall that M_2 is very large and thus the lightest chargino is heavy. $S1$ can be viewed as the best-case scenario for the like-sign dilepton signature because the gauge decay of the charged slepton leads in roughly 25% of the cases to the like-sign dilepton signature. The decay $\tilde{\ell} \to \ell \tilde{\chi}_1^0$ dominates for $\lambda' \lesssim 0.05(0.1)$ given a sufficiently large phase space of $\tilde{m} - m_{\tilde{\chi}_1^0} \gtrsim 100(250)$ GeV.

In the wino-like $\tilde{\chi}_1^0$ scenario, we have the three competing decays $\tilde{\ell}^+ \to u\bar{d}$, $\tilde{\ell} \to \ell \tilde{\chi}_1^0$ and $\tilde{\ell}^+ \to \bar{\nu} \tilde{\chi}_1^+$. The slepton

[2]Computationally, we increase M_1, M_2 or μ in the bino-, wino- or Higgsino-like $\tilde{\chi}_1^0$ scenario, respectively, while setting the decoupled mass parameters to 5 TeV.

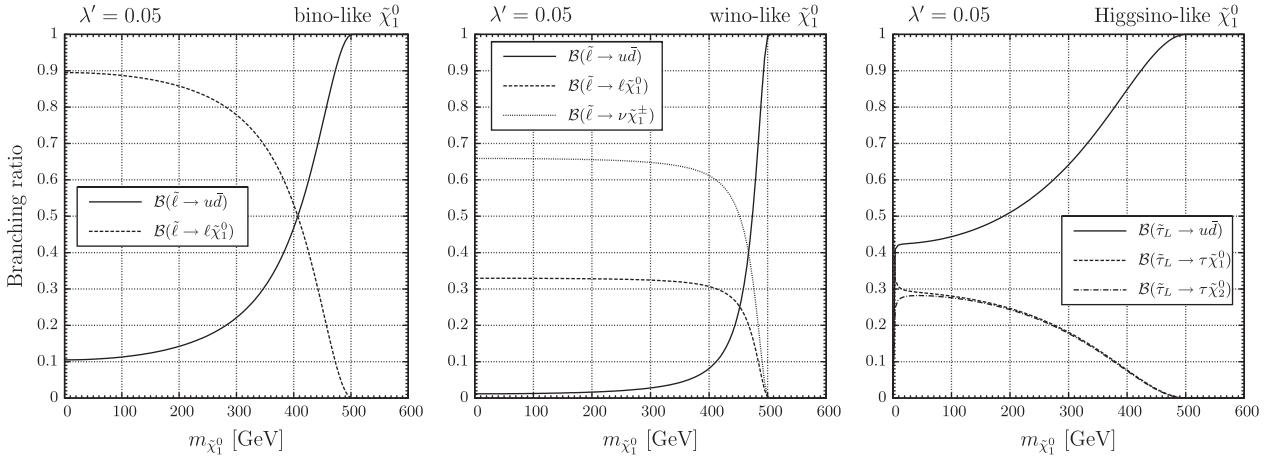

FIG. 4. Neutralino mass dependence of the branching ratios of the slepton decay modes in the bino-like (left), wino-like (middle) and Higgsino-like (right) $\tilde{\chi}_1^0$ scenarios. We chose a coupling strength of $\lambda' = 0.05$. The slepton mass is set to $\tilde{m} = 500$ GeV. The decays are calculated with ISAJET7.64 [88]. In the bino- and wino-like $\tilde{\chi}_1^0$ scenarios, the (purely left-handed) slepton can be $\tilde{\ell} = \tilde{e}_L, \tilde{\mu}_L, \tilde{\tau}_L$, while in the Higgsino-like $\tilde{\chi}_1^0$ scenario we only show the decays of a (purely left-handed) $\tilde{\tau}_L$. We set $\tan\beta = 10$.

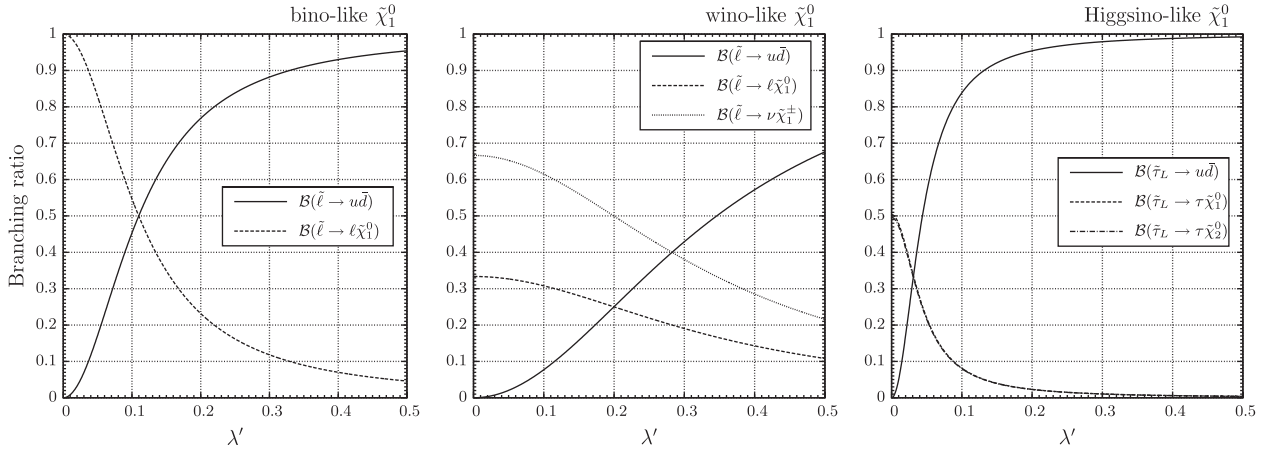

FIG. 5. λ' dependence of the branching ratios of the slepton decay modes in the bino-like (left panel), wino-like (middle) and Higgsino-like (right) $\tilde{\chi}_1^0$ scenarios. We chose a slepton mass of $\tilde{m} = 500$ GeV and a lightest neutralino mass of $m_{\tilde{\chi}_1^0} = 250$ GeV. The decays are obtained with ISAJET7.64 [88]. As in Fig. 4, the (purely left-handed) slepton can be $\tilde{\ell} = \tilde{e}_L, \tilde{\mu}_L, \tilde{\tau}_L$ in the bino- and wino-like $\tilde{\chi}_1^0$ scenario, while in the Higgsino-like $\tilde{\chi}_1^0$ scenario we only show the decays of a (purely left-handed) $\tilde{\tau}_L$. We set $\tan\beta = 10$.

decays twice as often to the chargino as to the neutralino, $\mathcal{B}(\tilde{\ell}^+ \to \bar{\nu}\tilde{\chi}_1^+) \approx 2\mathcal{B}(\tilde{\ell} \to \ell\tilde{\chi}_1^0)$. The gauge decays of the charged slepton therefore yield a like-sign dilepton signature only around $1/12$ of the time. The gauge decays dominate for $\lambda' \lesssim 0.05(0.35)$ for a mass difference of $m_{\tilde{\ell}} - m_{\tilde{\chi}_1^0} \gtrsim 50(250)$ GeV. They are slightly stronger than in the bino-like $\tilde{\chi}_1^0$ case due to the larger gauge coupling.

In the Higgsino-like $\tilde{\chi}_1^0$ scenario (the right panel in Figs. 4 and 5), we only give the branching ratios of the (left-handed)[3] third-generation slepton, $\tilde{\tau}_L$, because of the non-negligible Higgs Yukawa couplings. The gauge decays of the first- and second-generation sleptons are negligible. These thus only decay to dijets.

We therefore discuss the Higgsino-like $\tilde{\chi}_1^0$ scenario only for a left-handed $\tilde{\tau}_1$. For this, we set the ratio of the Higgs vacuum expectation values, $\tan\beta = 10$, which influences the τ Yukawa coupling. The branching ratios $\mathcal{B}(\tilde{\tau} \to \tau\tilde{\chi}_{1,2}^0)$ are roughly equal. The gauge decays of the stau yield a like-sign tau pair 50% of the time. However, they dominate the slepton decay modes only for a coupling $\lambda' \lesssim 0.01(0.04)$ for a given mass difference of $m_{\tilde{\ell}} - m_{\tilde{\chi}_1^0} \gtrsim 50(250)$ GeV.

In the case of the lightest stau, $\tilde{\tau}_1$, having a non-negligible right-handed component, the branching ratios get more complicated. The right-handed component does

[3]Here, we decoupled the soft-breaking right-handed stau mass parameter, $(m_{\tilde{\mathbf{E}}})_{33} = 5$ TeV, which leads to the lightest stau being purely left-handed.

not couple to the R-parity–violating operator but, via Yukawa interactions, to the chargino, leading to the decay $\tilde{\tau}_R^+ \to \bar{\nu}_\tau \tilde{\chi}_1^+$. Therefore, with increasing right-handedness of the $\tilde{\tau}_1$, on the one hand the R-parity–violating decay mode to two jets gets suppressed, while on the other hand the additional decay mode to the chargino decreases the (like-sign) dilepton rate. Recall that the production is also suppressed for a right-handed stau.

We do not further consider the Higgsino-like $\tilde{\chi}_1^0$ scenario. However, this analysis and the following results in Sec. III B show that a search for like-sign tau pairs would be able to probe resonantly produced tau sleptons with λ'_{3jk} $(j, k = 1, 2)$ even if the light gauginos, $\tilde{\chi}_{1,2}^0$ and $\tilde{\chi}_1^\pm$, are dominated by their Higgsino component.

III. SEARCHES AT THE LHC

In this section we use both the dijet and the like-sign dilepton signatures of resonant slepton production to constrain the R-parity–violating couplings λ'_{ijk} and the relevant slepton mass. For the calculation of both the R-parity–conserving and –violating sparticle decays we use ISAJET7.64 [88] and ISAWIG1.200 [89]. The ISAWIG output is fed into HERWIG6.510 [90–92] for the MC simulation at particle level. We simulate the response of the ATLAS and CMS detector using the general purpose detector simulation package DELPHES1.9 [93]. Jets are reconstructed using the anti-k_T algorithm [94,95]. In the dijet resonance search in Sec. III A, the distance parameter is set to $R = 0.6$ (ATLAS) and $R = 0.5$ (CMS), while we use $R = 0.4$ for the ATLAS like-sign dimuon search in Sec. III B. These jet definitions are in accordance with Refs. [21–23].

A. Search for dijet resonances

Both the ATLAS [21] and the CMS [22] experiments have searched for resonances in the dijet invariant mass spectrum using pp collision data corresponding to an integrated luminosity of 1.0 fb^{-1} at a center-of-mass energy of $\sqrt{s} = 7$ TeV. The nonobservation of new resonances led the experiments to derive limits for several new physics models including string resonances, exited quarks, axigluons and color octet scalar resonances. In the following, we use the model-independent limits on a fiducial signal cross section provided by ATLAS [21] and CMS [22] to constrain the resonant R-parity–violating production of sleptons [Eqs. (2) and (3)] with subsequent decay to two jets [Eqs. (4)(b) and (5)(b)]. The mass region in the ATLAS (CMS) search ranges from 0.9 (1) to 4.0 (4.1) TeV. Therefore, these searches can only constrain the resonant production of very heavy sleptons. Constraints for lower slepton masses have been derived from CDF and UA2 searches in [38].

In order to evaluate the acceptance of the analyses, we simulated 25 000 signal events for the process $pp \to \tilde{\ell}_i/\tilde{\nu}_i \to q_j q_k$ for each slepton mass, $\tilde{m}$. For the ATLAS search, we followed closely the prescription given in the Appendix of Ref. [21]. There, the limits are presented, assuming a certain width-to-mass ratio of the resonance, σ_G/m_G. In our study we determined σ_G/m_G with Gaussian fits of the dijet invariant mass distribution in the region between $0.8\tilde{m}$ and $1.2\tilde{m}$. It ranges from 8% to 5% for slepton masses from 0.9 GeV to 4 TeV. The acceptance $\mathcal{A}$ is given by the fraction of events lying in the region $0.8\tilde{m}$ to $1.2\tilde{m}$ (after all other kinematic requirements are applied) and ranges from 8.1% to 18.6% for slepton masses from 0.9 to 4 TeV.

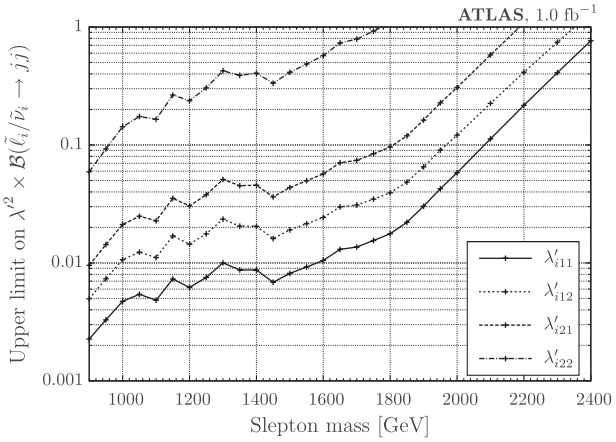

FIG. 6. Upper bounds on $\lambda'^2 \times \mathcal{B}(\tilde{\ell}_i/\tilde{\nu}_i \to jj)$ derived from the ATLAS dijet resonance searches with 1 fb^{-1} of data.

Both $\mathcal{A}$ and σ_G/m_G are fairly independent of $\lambda'_{ijk}(j, k \in \{1, 2\})$ for values between 0.001 and 1.0, since the resonance shape is dominated by the jet smearing of the detector simulation. Thus, we can easily derive upper limits on the R-parity–violating coupling squared times the branching ratio to dijets of the resonant slepton, $\lambda'^2 \times \mathcal{B}(\tilde{\ell}_i/\tilde{\nu}_i \to jj)$, for a given resonant slepton mass, $\tilde{m}$. These limits[4] are shown in Fig. 6 for the four types of couplings λ'_{i11}, λ'_{i12}, λ'_{i21} and λ'_{i22} $(i = 1, 2, 3)$. In the case of an intermediate third-generation slepton $(i = 3)$, the limit has to be multiplied by $\cos^2\theta_{\tilde{\tau}}$ to account for possible mixing in the stau sector. To be conservative, we reduced the signal by 7% to take into account the theoretical uncertainty of the NLO cross section prediction. The statistical uncertainty of the acceptance estimate is negligible.

The upper bounds on the four investigated R-parity–violating couplings, as derived from the ATLAS search, are listed together with $\mathcal{A}$ and σ_G/m_G in Table II in Appendix A. We only show upper limits for values $\lambda' < 1$ (perturbativity). For instance, assuming the decay to dijets being the only accessible decay mode, we can

[4]This analysis assumes that the sneutrino and the charged slepton resonance are not distinct. This is generally the case as long as the mass splitting is not too large, i.e. $m_{\tilde{\ell}} - m_{\tilde{\nu}} \lesssim \sigma_G \lesssim 10\% m_{\tilde{\ell}}$.

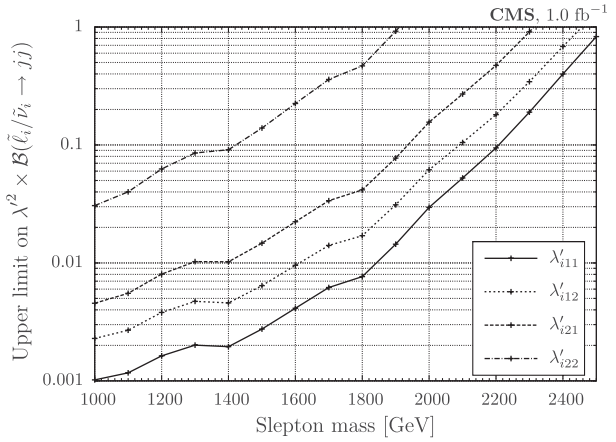

FIG. 7. Upper bounds on $\lambda'^2 \times \mathcal{B}(\tilde{\ell}_i/\tilde{\nu}_i \to jj)$ derived from the CMS dijet resonance searches with 1 fb^{-1} of data.

derive the upper bounds $\lambda'_{i11} \leq 0.07(0.09)$ and $\lambda'_{i22} \leq 0.38(0.64)$ for a slepton mass $\tilde{m} = 1000(1500)$ GeV.

In the CMS search [22], so-called wide jets are constructed based on anti-k_T jets with distance parameter $R = 0.5$. This allows us to distinguish between quark-quark (qq), quark-gluon (qg) and gluon-gluon (gg) dijet systems. Here, we employ the 95% C.L. upper limits on $\sigma \times \mathcal{A}$ derived for a qq dijet system. These limits only assume the natural resonance width to be small compared to the CMS dijet mass resolution.

We adopt the CMS construction of wide jets and apply the kinematic requirements to the jets. The acceptance is defined by the fraction of events with dijet invariant mass $m_{jj} > 838$ GeV. It ranges from 33.8% to 44.8% for slepton masses from 1.0 to 4.1 TeV. Again, we take into account a 7% systematic uncertainty on the signal.

In Fig. 7 we present the upper bounds on $\lambda'^2 \times \mathcal{B}(\tilde{\ell}_i/\tilde{\nu}_i \to jj)$ for the same couplings as before, but now derived from the CMS search. These results are given in detail in Table III in Appendix A. For a pure dijet decay of the slepton, $\mathcal{B}(\tilde{\ell}_i/\tilde{\nu}_i \to jj) \approx 100\%$, the upper bounds obtained are $\lambda'_{i11} \leq 0.03(0.05)$ and $\lambda'_{i22} \leq 0.18(0.37)$ for a slepton mass $\tilde{m} = 1000(1500)$ GeV. Due to the higher acceptance of the CMS search, these limits are considerably stricter than those obtained from the ATLAS search.

B. Search for prompt like-sign dimuons

We now turn to the discussion of the constraints from the like-sign dilepton signature. In Ref. [23] ATLAS searched for anomalous production of prompt like-sign muon pairs, using data corresponding to an integrated luminosity of 1.6 fb^{-1} at a center-of-mass energy of $\sqrt{s} = 7$ TeV. No significant excess was observed, and upper limits on the anomalous production of prompt like-sign muon pairs were derived. In the following section, we use these results to constrain the R-parity–violating couplings λ'_{2jk}, $j, k \in \{1, 2\}$, assuming the resonant production of a left-handed smuon, $\tilde{\mu}_L$ via Eq. (3), and its subsequent decay into the lightest neutralino, $\tilde{\chi}^0_1$, and a muon via Eq. (7)(a). The neutralino then decays as in Eq. (8) to the lepton with the same sign charge.

In the ATLAS search [23], the signal region is subdivided into four. The signal yield is defined by the number of like-sign muon pairs whose invariant mass, $m_{\mu\mu}$, is greater than 25, 100, 200, and 300 GeV, respectively. The main requirements on the muons are the following: The transverse momentum of the first (second) muon is larger then 20(10) GeV. Both muons are in the central region of the detector with pseudorapidity $|\eta| < 2.5$. They are separated from jets by $\Delta R(\mu, \text{jet}) > 0.4$, where jets are defined by the anti-k_t algorithm with a distance parameter of $R = 0.4$ and minimal transverse momentum $p_T(\text{jet}) > 7$ GeV. The muons have to be prompt (originating from the primary vertex). This translates in our case into a requirement on the slepton lifetime to be less than $\tau < 10^{-14}$ s. Furthermore, we employ the same cone isolation criteria for the muons as in the ATLAS note [23].

We now discuss the kinematic properties of single slepton production at the LHC with 7 TeV center-of-mass energy. The slepton is forced to decay into the lightest neutralino, i.e. we consider the process[5] $pp \to \tilde{\ell}^*/\tilde{\nu}^* \to (\mu/\nu)\tilde{\chi}^0_1$. In Fig. 8(a) we provide the transverse momentum (p_T) distribution of the muons passing the isolation, pseudorapidity, jet separation and minimal transverse momentum ($p_T \geq 10$ GeV) constraints, whereas Fig. 8(b) gives the invariant mass distribution[6] of the like-sign dimuon pairs after the full event selection (except the final $m_{\mu\mu}$ requirement). We give these distributions for three example models with different lightest neutralino masses $m_{\tilde{\chi}^0_1} = (100, 250, 400)$ GeV, slepton mass $\tilde{m} = 500$ GeV and a nonzero R-parity–violating coupling λ'_{2jk}.

For large mass splittings between the slepton and the neutralino, $\Delta m = \tilde{m} - m_{\tilde{\chi}^0_1}$, we can identify two distinct peaks in the muon-p_T spectrum. In the first model considered ($\tilde{m} = 500$ GeV, $m_{\tilde{\chi}^0_1} = 100$ GeV), we have hard muons with typical p_T values around 200–250 GeV. These muons originate from the slepton decay. In contrast, the soft muons accumulating at the low end of the distribution stem from the three-body decay of the neutralino (and the chargino in the wino-like scenario).

For larger neutralino masses (second and third models) the phase space for the muons from the gaugino decay increases, leading to the migration of the left peak in the p_T distribution towards higher values. On the other hand, the

[5]We must include the sneutrino production even though it does not lead to like-sign dileptons. Both production processes are jointly encoded in HERWIG6.510.

[6]Both distributions in Fig. 8 are obtained from Monte Carlo simulation using the bino-like $\tilde{\chi}^0_1$ scenario, normalized to unity for a bin size of 2 GeV and then smoothened for better visualization.

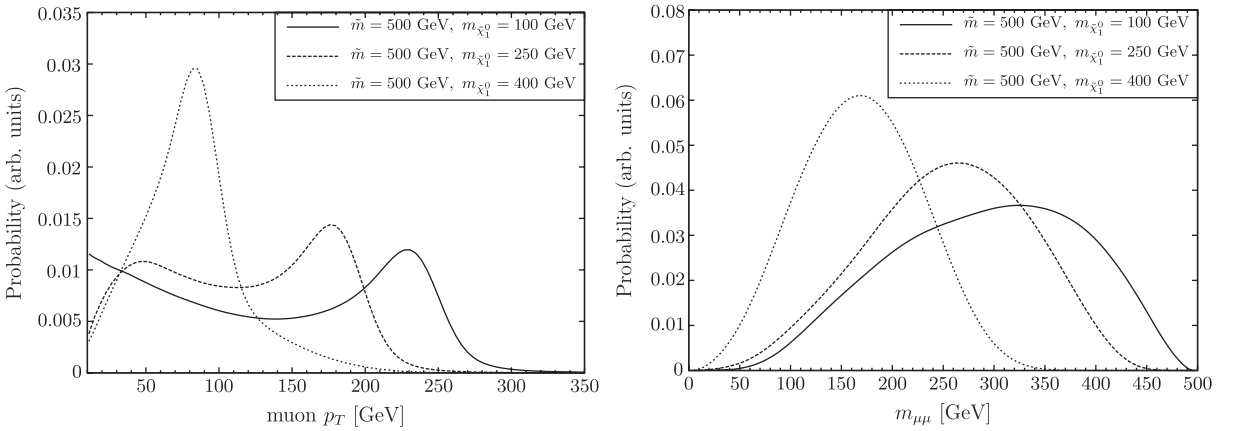

(a) p_T distribution of the isolated muons. (b) Invariant mass distribution of the like–sign dimuon pairs.

FIG. 8. Kinematic properties of the single slepton production process $pp \to \tilde{\ell}^*/\tilde{\nu}^* \to \mu/\nu\tilde{\chi}_1^0$ via λ'_{2jk} at the LHC with a center-of-mass energy of 7 TeV: (a) transverse momentum distribution of the muons passing the object selection (isolation, $p_T > 10$ GeV) of Ref. [23]; (b) invariant mass distribution of the like-sign dimuon pairs which pass the full event selection. The slepton mass is set to $\tilde{m} = 500$ GeV. We show the shapes for three different neutralino masses, $m_{\tilde{\chi}_1^0} = (100, 250, 500)$ GeV.

muons from the slepton decay become softer due to the smaller Δm. In the third model considered ($\tilde{m} = 500$ GeV, $m_{\tilde{\chi}_1^0} = 400$ GeV), the peaks overlap at a p_T value of around 80–90 GeV. For even smaller Δm, the muons from the slepton decay will constitute the low end of the p_T spectrum.

The invariant mass distribution of the like-sign dimuon pairs shown in Fig. 8(b) exhibits a broad peak of approximately Gaussian shape. The peak value increases for larger mass splitting Δm.

From this discussion, we can already predict that the acceptance of the ATLAS like-sign dimuon search will decrease (i) for small neutralino masses and (ii) in the small Δm region, where the slepton and the neutralino are close in mass. In both cases, one of the muons is rather soft due to reduced phase space and thus may not fulfill the minimum p_T requirement. This is especially important for (i), since the neutralino decays via a three-body decay. On the other hand, in (ii), the invariant mass $m_{\mu\mu}$ tends to be small, thus reducing in particular the acceptance of the high $m_{\mu\mu}$ signal regions.

The (normalized) distributions in Fig. 8 are to a good approximation independent of the choice of j, k and the value of λ'_{2jk} (as long as it is a prompt neutralino decay). Furthermore, they are independent of whether we have a bino- or wino-like $\tilde{\chi}_1^0$ scenario.[7] However, note that the absolute number of like-sign dimuon pairs is different for the scenarios $S1$ and $S2$; cf. Sec. II B.

[7]In the case of a Higgsino-like $\tilde{\chi}_1^0$, one of the peaks in the lepton-p_T spectrum would be more pronounced since we get twice as many leptons from the neutralino decays compared to the bino- and wino-like $\tilde{\chi}_1^0$ scenarios.

The signal acceptance $\mathcal{A}$ of the like-sign prompt dimuon search is evaluated by simulating the process $pp \to \tilde{\ell}^*/\tilde{\nu}^* \to (\mu/\nu)\tilde{\chi}_1^0$ in HERWIG6.510. We simulated 5000 events for each point in the $(m_{\tilde{\chi}_1^0}, \tilde{m})$ mass plane, where we use step sizes of $\Delta\tilde{m} = 10$ GeV and $\Delta m_{\tilde{\chi}_1^0} = 20$ GeV. For $m_{\tilde{\chi}_1^0} \leq 40$ GeV (light neutralino) and $m_{\tilde{\chi}_1^0} \in \{\tilde{m} - 40\ \text{GeV}, \tilde{m}\}$ (boundary region), we decrease the neutralino mass step size to $\Delta m_{\tilde{\chi}_1^0} = 5$ GeV since the acceptance is rapidly changing in these regions. The acceptance maps of the four signal regions ($m_{\mu\mu} > 25, 100, 200, 300$ GeV) are given in Fig. 11 in Appendix B. For large parts of the $(m_{\tilde{\chi}_1^0}, \tilde{m})$ mass plane, the acceptance $\mathcal{A}$ lies between 2% and 7%. However, in the regions with low neutralino masses, $m_{\tilde{\chi}_1^0} \lesssim$ (100–200) GeV, and in the region with small $\Delta m = \tilde{m} - m_{\tilde{\chi}_1^0}$, the search becomes insensitive ($\mathcal{A} \lesssim 2\%$), as expected from the discussion above. More details are given in Appendix B.

The branching ratios $\mathcal{B}(\tilde{\ell} \to \ell\tilde{\chi}_1^0)$ and $\mathcal{B}(\tilde{\nu} \to \nu\tilde{\chi}_1^0)$ are calculated with ISAJET7.64 in the same grid for different values of λ' for both the bino- and wino-like $\tilde{\chi}_1^0$ scenarios.

The expected signal rate for a given coupling λ'_{2jk} and masses $\tilde{m}$, $m_{\tilde{\chi}_1^0}$ is calculated by

$$[\sigma^{\text{NLO}}(\tilde{\ell} \to \ell\tilde{\chi}_1^0) \times \mathcal{B}(\tilde{\ell} \to \ell\tilde{\chi}_1^0) + \sigma^{\text{NLO}}(\tilde{\nu} \to \nu\tilde{\chi}_1^0) \times \mathcal{B}(\tilde{\nu} \to \nu\tilde{\chi}_1^0)] \times \mathcal{A}(\tilde{m}, m_{\tilde{\chi}_1^0}), \quad (12)$$

where the branching ratios encode the model dependence (on the bino- or wino-like $\tilde{\chi}_1^0$ scenario). The 95% C.L. upper limits on the fiducial cross section for

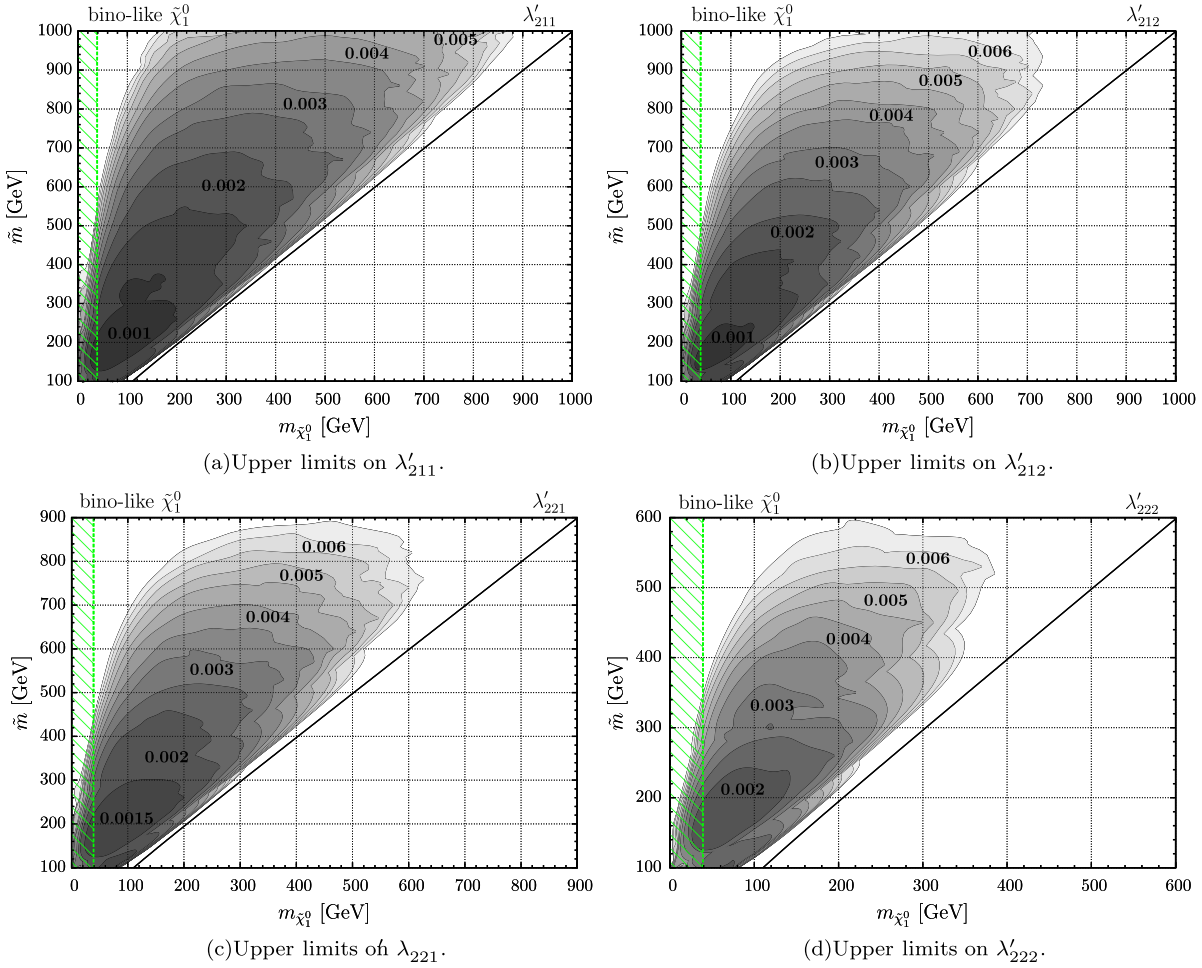

(a)Upper limits on λ'_{211}. (b)Upper limits on λ'_{212}.

(c)Upper limits on λ_{221}. (d)Upper limits on λ'_{222}.

FIG. 9 (color online). Upper bounds on $\lambda'_{2jk}(j, k \in \{1, 2\})$ in the $(m_{\tilde{\chi}_1^0}, \tilde{m})$ mass plane in the bino-like $\tilde{\chi}_1^0$ scenario, derived from the ATLAS prompt like-sign dimuon search. The contour levels are given in steps of 0.0005. The green striped region is excluded due to the lower mass bound from LEP on the lightest neutralino, $m_{\tilde{\chi}_1^0} \geq 39$ GeV [65,66].

like-sign dimuon production provided by ATLAS are 170.24, 15.68, 4.76, and 2.8 fb for the signal regions $m_{\mu\mu} > 25$, 100, 200, and 300 GeV, respectively [23]. If the signal rate, Eq. (12), exceeds the limit in at least one of the signal regions, we consider the model to be excluded.

We estimate the total uncertainty of the theory prediction to be 10%, taking into account a 5% systematic uncertainty for the parton density functions, 3% from factorization and renormalization scale uncertainties of the NLO cross section [30], and an averaged statistical uncertainty of the acceptance estimate.[8] In order to be conservative, we reduce our signal estimate by the 10% uncertainty in the limit setting procedure.

We present the upper limits[9] on the four investigated R-parity–violating couplings $\lambda'_{2jk}(j, k \in \{1, 2\})$ within the bino-like $\tilde{\chi}_1^0$ scenario ($S1$) in Fig. 9. They are presented as contours in the $(m_{\tilde{\chi}_1^0}, \tilde{m})$ mass plane. The green striped region indicates the LEP lower mass limit on the lightest neutralino, $m_{\tilde{\chi}_1^0} \geq 39$ GeV [65,66]. Note that this limit (and the limit on the chargino mass) is parameter dependent; cf. Sec. I.

The derived upper bounds on λ' range from 0.001 (dark) to 0.0065 (bright) and are displayed in steps of 0.0005 in gray scale. Since the single slepton production cross section decreases with the slepton mass, the bounds become

[8]With 5000 simulated events, the relative statistical uncertainty on a typical value of the acceptance $\mathcal{A} = 1\%(7\%)$ is $\Delta\mathcal{A} = 14\%(5\%)$.

[9]Due to our rather simple treatment of the systematic uncertainties of the signal, we cannot claim our upper limits to be exactly at 95% C.L. In fact, due to the conservative approach of subtracting the systematic uncertainty from the signal yield, we expect our upper limit to be "at 95% C.L. or more."

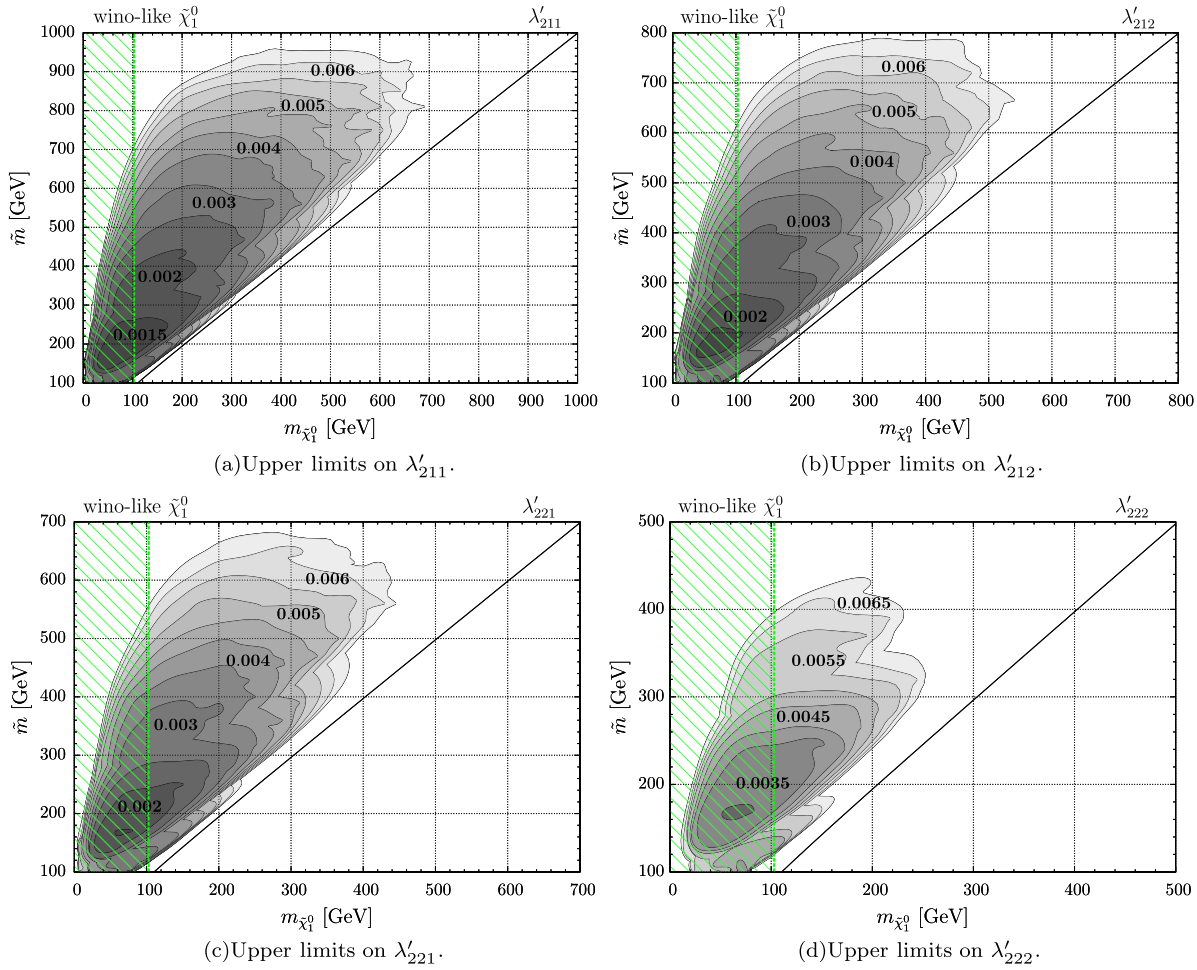

(a)Upper limits on λ'_{211}. (b)Upper limits on λ'_{212}.

(c)Upper limits on λ'_{221}. (d)Upper limits on λ'_{222}.

FIG. 10 (color online). Upper bounds on $\lambda'_{2jk}(j, k \in \{1, 2\})$ in the $(m_{\tilde{\chi}_1^0}, \tilde{m})$ mass plane in the wino-like $\tilde{\chi}_1^0$ scenario, derived from the ATLAS prompt like-sign dimuon search. The contour levels are given in steps of 0.0005. The green shaded region is excluded due to the lower mass bound from LEP on the lightest chargino, $m_{\tilde{\chi}_1^\pm} \geq 103$ GeV [65,66], which is nearly mass degenerate with the lightest neutralino in these scenarios.

weaker for heavier smuons. Also, due to the insensitivity of the like-sign dimuon search in the regions of low neutralino mass and low $\Delta m = \tilde{m} - m_{\tilde{\chi}_1^0}$, we cannot obtain upper bounds on λ' in these regions.

The most stringent limits are obtained for the coupling λ'_{211} due to the larger cross section; cf. Fig. 1. For a roughly elliptic region with $m_{\tilde{\chi}_1^0} \sim \tilde{m} - 100$ GeV and $\tilde{m} \sim (150\text{–}300)$ GeV, we obtain $\lambda'_{211} \leq 0.001$. Even for large smuon masses of $\lesssim \mathcal{O}(1$ TeV), we can still derive bounds down to $\lambda'_{211} \lesssim 0.0045$. The other couplings are less constrained due to the smaller cross section; cf. Sec. II A. The weakest bounds are therefore set on λ'_{222}, ranging from 0.002 for $(m_{\tilde{\chi}_1^0}, \tilde{m}) \sim (100, 200)$ GeV to 0.0065 for smuon masses $\tilde{m} \lesssim 550$ GeV.

We now turn to the discussion of the results in the wino-like $\tilde{\chi}_1^0$ scenario ($S2$) shown in Fig. 10. The LEP lower mass limit on the chargino, $m_{\tilde{\chi}_1^\pm} \geq 103$ GeV [65,66], is indicated by the green striped region. As discussed in Sec. II B, we expect like-sign dimuon events to result from the charged slepton gauge decays only 1/12 of the time. Thus, the upper limits on the R-parity–violating coupling λ' are weaker. For instance, for light smuon and neutralino masses, $(m_{\tilde{\chi}_1^0}, \tilde{m}) = (100, 200)$ GeV, the upper bounds obtained in the wino-like $\tilde{\chi}_1^0$ scenario are λ'_{211}, $\lambda'_{212} \leq 0.0015$, $\lambda'_{221} \leq 0.002$ and $\lambda'_{222} \leq 0.0035$.

The bino-like and wino-like $\tilde{\chi}_1^0$ limits can be interpreted as the best-case and worst-case scenarios, respectively, for the like-sign dilepton signature. These new limits improve current limits from the Tevatron [39,40] on λ'_{211} by a factor $\mathcal{O}(40)$ or more.

We do not consider a Higgsino-like lightest neutralino ($S3$). As discussed in Sec. II B, the slepton decay to the Higgsino-like $\tilde{\chi}_1^0$, $\tilde{\chi}_2^0$ and $\tilde{\chi}_1^\pm$ is highly suppressed due to the small Yukawa coupling, and the competing

R-parity–violating decay $\tilde{\mu} \to jj$ would dominate, leading to an overall suppression of the like-sign dimuon signature. However, we want to remark that exploring the Higgsino-like $\tilde{\chi}_1^0$ scenario with R-parity–violating couplings λ'_{3jk} and a resonantly produced (left-handed) $\tilde{\tau}_1$ would be feasible with a like-sign ditau search.

IV. CONCLUSIONS

We have investigated the impact of LHC data on the resonant production of single sleptons in R-parity–violating models. We presented the NLO production cross section for resonant sleptons in pp collisions at 7 TeV center-of-mass energy. We then discussed the decay modes of the slepton for three simplified models, where the lightest neutralino is either bino- ($S1$), wino- ($S2$), or Higgsino-like ($S3$). We estimated the event yield with a like-sign dilepton final state. Although these scenarios are simplified, they still represent wide regions of (realistic) grand unified theory-based SUSY breaking scenarios like the CMSSM or the anomaly-mediated SUSY breaking, as long as the assumed (relevant) sparticle mass hierarchy is fulfilled.

The main part of this work focused on the derivation of upper bounds on the R-parity–violating couplings from recently published LHC results. First, we considered the dijet signature of resonant sleptons. Using ATLAS and CMS dijet searches each with 1 fb^{-1} of data, we derived upper bounds on the R-parity–violating coupling squared, λ'^2_{ijk} ($i = 1, 2, 3$, $j, k = 1, 2$), times the branching fraction of the slepton to dijets. These limits depend only on the mass of the resonant slepton, $\tilde{m}$, and are thus complementary to low-energy upper bounds, which usually scale with the squark masses. The limits derived from the CMS search turn out to be considerably stricter than those of ATLAS. If the dijet channel is the dominant decay mode, $\mathcal{B}(\tilde{\ell}_i/\tilde{\nu}_i \to jj) \approx 100\%$, the upper bounds obtained are, for instance, $\lambda'_{i11} \leq 0.03(0.05)$ and $\lambda'_{i22} \leq 0.18(0.37)$ for a slepton mass $\tilde{m} = 1000(1500)$ GeV. The complete ATLAS and CMS results are listed in Tables II and III, respectively. However, these limits from LHC dijet resonance searches only apply for a very massive spectrum where the slepton mass is in the range 0.9 TeV $\leq \tilde{m} \leq$ 2.5 TeV, since a dijet resonance search in the lower mass region is still insensitive due to the overwhelming QCD background.

We then studied the like-sign dilepton signature, which is a very promising channel for resonant slepton production due to the small SM background. Using an ATLAS search for anomalous like-sign dimuon pairs with 1.6 fb^{-1} of data, we set limits on λ'_{211}, λ'_{212}, λ'_{221} and λ'_{222} in the lightest neutralino-slepton mass plane, $(m_{\tilde{\chi}_1^0}, \tilde{m})$, assuming a bino-like ($S1$) or wino-like ($S2$) lightest neutralino LSP. These bounds range from 0.001 (for low slepton and neutralino masses $\sim$100 GeV to 300 GeV in $S1$) to 0.0065 (heavier slepton and lightest neutralino masses up to 1 TeV). The strictest bounds are obtained for the λ'_{211} coupling for a bino-like lightest neutralino ($S1$). Our results improve the bounds on λ'_{211} obtained from the Tevatron by a factor $\gtrsim \mathcal{O}(40)$. For instance, for a slepton mass $\tilde{m} = 300(400)$ GeV and a neutralino mass $m_{\tilde{\chi}_1^0} = 150(200)$ GeV, the upper bound $\lambda'_{211} < 0.04(0.08)$ obtained by D0 [39,40] has improved to 0.001(0.0015) by our analysis of the LHC data.

Furthermore, we discussed in some detail the performance of the ATLAS like-sign dimuon search on the resonant slepton signal. For this, we presented the p_T distribution of the isolated muons and the like-sign dimuon invariant mass distribution for three different mass configurations [$\tilde{m} = 500$ GeV, $m_{\tilde{\chi}_1^0} = (100, 250, 400)$ GeV]. The signal acceptance is reduced (i) for small neutralino masses and (ii) for a low mass difference between the slepton and the lightest neutralino. In either case, one of the muons has a rather low transverse momentum.

We want to remark that scalar leptoquark searches at ATLAS [96] and CMS [97] are also sensitive to resonant slepton production. These analyses searched for two jets associated with either two leptons or one lepton and missing energy (coming from a neutrino). As discussed in Sec. II B, this is also a typical signature of resonant slepton production. Furthermore, the analyses with one final state lepton should perform better than the (like-sign) dilepton search in the parameter region of small mass difference between the slepton and the lightest neutralino, where the lepton detection efficiency is low due to reduced phase space.

We also want to encourage the ATLAS and CMS Collaborations to perform a similar search for like-sign ditau pairs. This would shed new light on the R-parity–violating couplings $\lambda'_{3ij}(i, j = 1, 2)$ assuming a resonantly produced $\tilde{\tau}_1$ with a non-negligible left-handed component.

ACKNOWLEDGMENTS

We thank Sebastian Grab for helpful discussions, reading the manuscript, and providing the code for the NLO cross section computation. Furthermore, we are grateful to Phillip Bechtle, Till F. Eifert, Karl Jacobs and Peter Wienemann for their help on experimental questions. This work was partially funded by the Helmholtz Alliance "Physics at the Terascale" and by the BMBF "Verbundprojekt HEP-Theorie" under Contract No. 0509PDE. T. S. thanks the Bonn-Cologne Graduate School of Physics and Astronomy for additional financial support.

APPENDIX A: ADDITIONAL TABLES FOR THE DIJET RESONANCE SEARCH RESULTS

The results of the dijet resonance study in Sec. III A are listed in Tables II and III for the ATLAS and CMS analyses, respectively. The upper bounds on the R-parity–violating coupling squared times the branching ratio of the slepton to dijets, $\lambda'^2_{ijk} \times \mathcal{B}(\tilde{\ell}_i/\tilde{\nu}_i \to jj)$, are presented

for all $j,\ k \in \{1,2\}$ separately up to the perturbativity bound. We also give the signal acceptance $\mathcal{A}$ for each slepton mass $\tilde{m}$, which has been evaluated with our MC simulation. For the ATLAS results, Table II, we also provide the resonance width to mass ratio, σ_G/m_G, as derived from a Gaussian fit to the resonance.

APPENDIX B: SIGNAL ACCEPTANCE OF THE PROMPT LIKE-SIGN DIMUON SEARCH

In Fig. 11 we give the signal acceptance in the $(m_{\tilde{\chi}_1^0},\ \tilde{m})$ mass plane for each signal region ($m_{\mu\mu} > 25$, 100, 200, 300 GeV) of the ATLAS prompt like-sign dimuon search [23] for the simulated process $pp \to \tilde{\ell}^*/\tilde{\nu}^* \to (\mu/\nu)\tilde{\chi}_1^0$.

For most of the parameter space, the acceptance ranges between 2% and 7%, where the highest values are obtained for models with $m_{\tilde{\chi}_1^0} \approx \tilde{m}/2$. In that case, neither the slepton nor the neutralino decay is kinematically suppressed, leading to sizable transverse momenta of the two leptons. In contrast, the regions with either a low neutralino mass or a low mass difference between slepton and lightest neutralino, $\Delta m = \tilde{m} - m_{\tilde{\chi}_1^0}$, feature a very small acceptance. Here, one of the leptons is soft due to reduced phase space, as discussed in Sec. III B, and therefore fails to pass the minimum p_T requirement.

The insensitive region at low neutralino masses does not depend on the specific $m_{\mu\mu}$ requirement, since it typically features higher values of $m_{\mu\mu}$; cf. Fig. 8(b). In contrast, the acceptance in the low Δm region highly depends on the $m_{\mu\mu}$ cut. Decreasing the mass difference Δm leads to a shift of the $m_{\mu\mu}$ distribution towards lower values. Thus, only the $m_{\mu\mu} > 25$ GeV signal region is capable of exploring the parameter region with Δm down to ≈ 10 GeV, while the other signal regions with $m_{\mu\mu} > (100, 200, 300)$ GeV require a mass difference of $\Delta m \gtrsim (20, 75, 150)$ GeV, respectively, to become sensitive (i.e. to obtain $\mathcal{A} \gtrsim 2\%$).

TABLE II. Upper limits on $\lambda'^2 \times \mathcal{B}(\tilde{\ell}_i/\tilde{\nu}_i \to jj)$ derived from the ATLAS search for dijet resonances. The first column gives the resonant slepton mass, $\tilde{m}$ (in GeV), and the second and third columns show the acceptance $\mathcal{A}$ (in %) and the width-to-mass ratio, σ_G/m_G (in %), of the Gaussian resonance fit, respectively. The other columns contain the upper limits on $\lambda'^2 \times \mathcal{B}(\tilde{\ell}_i/\tilde{\nu}_i \to jj)$, where the indices of λ' are indicated in the table header ($i = 1, 2, 3$).

			Upper limits on $\lambda'^2_{ijk} \times \mathcal{B}(\tilde{\ell}_i/\tilde{\nu}_i \to jj)$			
$\tilde{m}$ [GeV]	$\mathcal{A}$ (in%)	σ_G/m_G (in%)	$i11$	$i12$	$i21$	$i22$
900	8.1	8.1	0.00226	0.00497	0.00953	0.05931
950	8.0	7.2	0.00329	0.00734	0.01432	0.09274
1000	7.9	7.5	0.00473	0.01067	0.02117	0.14252
1050	8.2	7.3	0.00542	0.01234	0.02490	0.17413
1100	7.9	6.3	0.00483	0.01110	0.02275	0.16507
1150	8.6	7.9	0.00731	0.01694	0.03524	0.26513
1200	8.8	6.8	0.00619	0.01442	0.03045	0.23733
1250	8.8	6.5	0.00754	0.01764	0.03779	0.30482
1300	8.6	7.5	0.01002	0.02349	0.05104	0.42574
1350	9.0	7.0	0.00873	0.02051	0.04516	0.38927
1400	9.0	7.5	0.00871	0.02044	0.04560	0.40587
1450	9.1	6.4	0.00686	0.01608	0.03634	0.33384
1500	9.1	6.5	0.00815	0.01904	0.04358	0.41282
1550	9.3	6.3	0.00924	0.02149	0.04976	0.48586
1600	9.5	6.3	0.01050	0.02426	0.05683	0.57162
1650	9.4	6.4	0.01303	0.02987	0.07077	0.73286
1700	9.8	6.3	0.01364	0.03098	0.07419	0.79059
1750	9.4	6.1	0.01547	0.03478	0.08418	0.92254
1800	9.6	6.4	0.01769	0.03929	0.09605	⋯
1850	9.8	5.9	0.02210	0.04840	0.11951	⋯
1900	9.8	7.0	0.03023	0.06522	0.16255	⋯
1950	10.0	6.6	0.04261	0.09040	0.22733	⋯
2000	10.0	6.0	0.05815	0.12116	0.30730	⋯
2100	10.2	6.5	0.11257	0.22523	0.58045	⋯
2200	10.4	5.9	0.21673	0.41398	⋯	⋯
2300	10.5	6.3	0.41049	0.74428	⋯	⋯
2400	10.6	5.7	0.76454	⋯	⋯	⋯

TABLE III. Upper limits on $\lambda'^2 \times \mathcal{B}(\tilde{\ell}_i/\tilde{\nu}_i \to jj)$ derived from the CMS search for narrow dijet resonances. The first column gives the resonant slepton mass, $\tilde{m}$ (in GeV), and the second shows the acceptance $\mathcal{A}$ (in %). The other columns contain the upper limits on $\lambda'^2 \times \mathcal{B}(\tilde{\ell}_i/\tilde{\nu}_i \to jj)$, where the indices of λ' are indicated in the table header ($i = 1, 2, 3$).

		Upper limits on $\lambda'^2_{ijk} \times \mathcal{B}(\tilde{\ell}_i/\tilde{\nu}_i \to jj)$			
$\tilde{m}$ [GeV]	$\mathcal{A}$ (in%)	$i11$	$i12$	$i21$	$i22$
1000	33.8	0.00102	0.00229	0.00455	0.03064
1100	34.8	0.00117	0.00269	0.00552	0.04007
1200	35.7	0.00163	0.00380	0.00803	0.06254
1300	35.7	0.00201	0.00472	0.01026	0.08555
1400	36.6	0.00195	0.00458	0.01023	0.09103
1500	36.6	0.00275	0.00642	0.01469	0.13914
1600	37.3	0.00413	0.00954	0.02235	0.22478
1700	37.3	0.00619	0.01407	0.03370	0.35911
1800	38.1	0.00766	0.01701	0.04160	0.46863
1900	37.6	0.01441	0.03108	0.07747	0.92097
2000	38.2	0.02956	0.06159	0.15622	...
2100	38.6	0.05246	0.10497	0.27053	...
2200	38.2	0.09454	0.18058	0.47210	...
2300	39.0	0.18974	0.34403	0.91070	...
2400	39.1	0.39971	0.68404	...	...
2500	39.1	0.82990	...	...	...

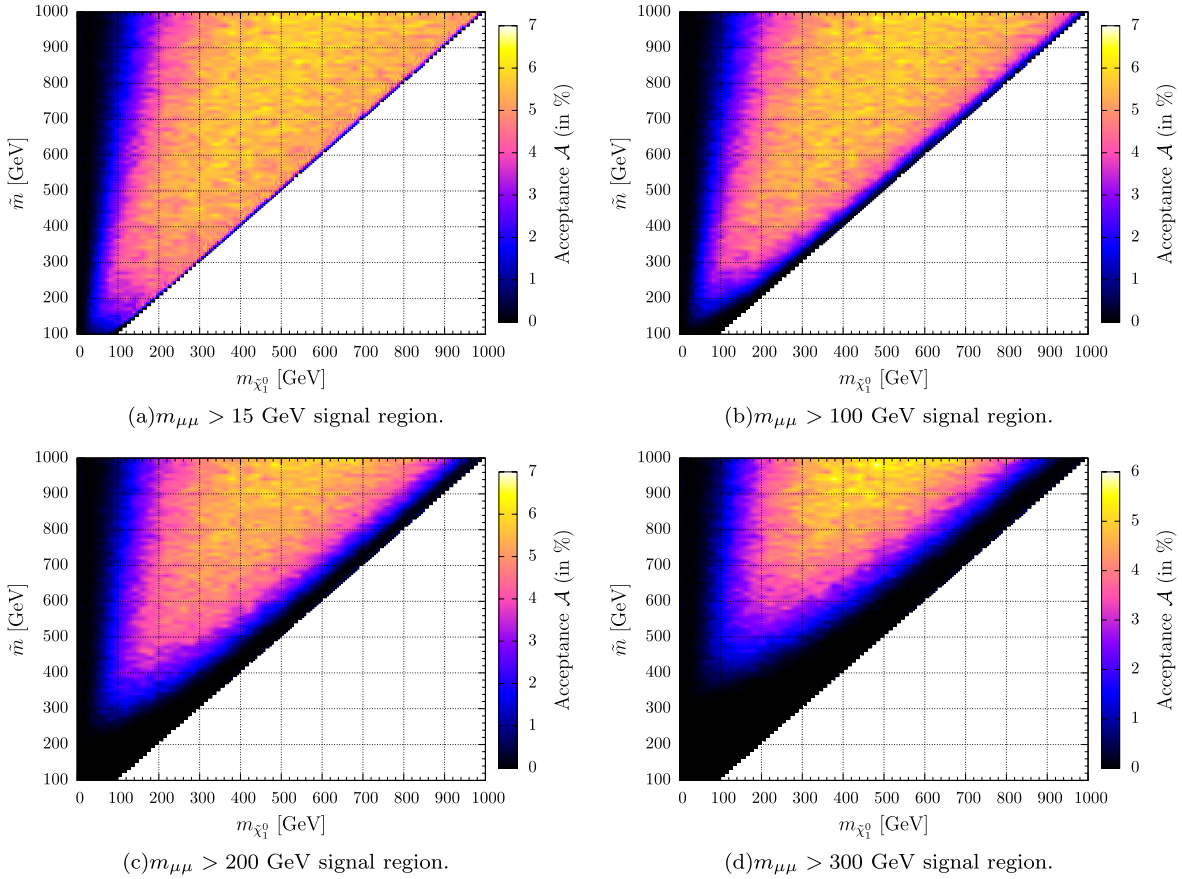

(a)$m_{\mu\mu} > 15$ GeV signal region.

(b)$m_{\mu\mu} > 100$ GeV signal region.

(c)$m_{\mu\mu} > 200$ GeV signal region.

(d)$m_{\mu\mu} > 300$ GeV signal region.

FIG. 11 (color online). Signal acceptance $\mathcal{A}$ of the ATLAS same-sign prompt dimuon search for the resonant slepton production process $pp \to \tilde{\ell}^*/\tilde{\nu}^* \to (\mu/\nu)\tilde{\chi}^0_1$. (a)–(d) show the four signal regions with $m_{\mu\mu} > (25, 100, 200, 300)$ GeV, respectively.

Furthermore, in order to obtain a large $m_{\mu\mu}$ value, the slepton mass $\tilde{m}$ has to be sufficiently large. Thus, the signal regions with $m_{\mu\mu} > (25, 100, 200, 300)$ GeV become sensitive for slepton masses $\tilde{m} \gtrsim (125, 200, 330, 500)$ GeV, respectively.

Although the $m_{\mu\mu} \geq 25$ GeV selection has the best acceptance coverage, it is still important to use the other signal regions also, because they have less SM background and thus stricter upper limits on the fiducial cross section. In parameter regions with heavier sleptons $\tilde{m} \gtrsim \mathcal{O}(600\ \text{GeV})$ and neutralino masses around $\tilde{m}/2$, the signal region with $m_{\mu\mu} > 300$ GeV typically poses the strictest limits on the R-parity–violating couplings.

[1] During the first run, however, there was a problem: Ingo Ansbach, *Zwielicht zum Preis von einem: Gedichte* (Verlag Liber Libri Wien/Pegasus Lyrik, Auflage, 2009).

[2] For reviews on supersymmetry, see for example: H. P. Nilles, Phys. Rep. **110**, 1 (1984); H. E. Haber and G. L. Kane, Phys. Rep. **117**, 75 (1985); M. Drees, arXiv:hep-ph/9611409; S. P. Martin, in *Perspectives on Supersymmetry II*, edited by G. L. Kane (World Scientific, Singapore, 2011), pp. 1–153.

[3] G. R. Farrar and P. Fayet, Phys. Lett. **76B**, 575 (1978).

[4] G. Aad *et al.* (ATLAS Collaboration), Phys. Lett. B **710**, 67 (2012); Phys. Rev. D **85**, 012006 (2012); J. High Energy Phys. 11 (2011) 099; Phys. Lett. B **709**, 137 (2012); **710**, 519 (2012); Phys. Rev. Lett. **108**, 181802 (2012).

[5] S. Chatrchyan *et al.* (CMS Collaboration), Phys. Rev. Lett. **106**, 211802 (2011); J. High Energy Phys. 06 (2011) 026; 06 (2011) 077; 06 (2011) 093; 07 (2011) 113; 08 (2011) 155; Phys. Rev. D **85**, 012004 (2012); J. High Energy Phys. 08 (2011) 156; Phys. Rev. Lett. **107**, 221804 (2011).

[6] P. Bechtle, B. Sarrazin, K. Desch, H. K. Dreiner, P. Wienemann, M. Kramer, C. Robens, and B. O'Leary, Phys. Rev. D **84**, 011701 (2011); O. Buchmueller *et al.*, Eur. Phys. J. C **72**, 1878 (2012); B. C. Allanach, T. J. Khoo, C. G. Lester, and S. L. Williams, J. High Energy Phys. 06 (2011) 035; S. Sekmen, S. Kraml, J. Lykken, F. Moortgat, S. Padhi, L. Pape, M. Pierini, H. B. Prosper, and M. Spriopulu, J. High Energy Phys. 02 (2012) 075; A. Arbey, M. Battaglia, and F. Mahmoudi, Eur. Phys. J. C **72**, 1847 (2012).

[7] H. K. Dreiner, in *Perspectives on Supersymmetry II*, edited by G. L. Kane (World Scientific, Singapore, 2011), pp. 565–583.

[8] B. C. Allanach, A. Dedes, and H. K. Dreiner, Phys. Rev. D **69**, 115002 (2004); **60**, 056002 (1999).

[9] H. K. Dreiner, C. Luhn, and M. Thormeier, Phys. Rev. D **73**, 075007 (2006); L. E. Ibanez and G. G. Ross, Phys. Lett. B **260**, 291 (1991).

[10] M. Hirsch, M. A. Diaz, W. Porod, J. C. Romao, and J. W. F. Valle, Phys. Rev. D **62**, 113008 (2000).

[11] H. K. Dreiner and M. Thormeier, Phys. Rev. D **69**, 053002 (2004).

[12] L. J. Hall and M. Suzuki, Nucl. Phys. **B231**, 419 (1984).

[13] S. Davidson and M. Losada, J. High Energy Phys. 05 (2000) 021.

[14] H. K. Dreiner, M. Hanussek, and S. Grab, Phys. Rev. D **82**, 055027 (2010).

[15] P. Minkowski, Phys. Lett. **67B**, 421 (1977).

[16] R. N. Mohapatra and G. Senjanovic, Phys. Rev. Lett. **44**, 912 (1980).

[17] H. K. Dreiner, C. Luhn, H. Murayama, and M. Thormeier, Nucl. Phys. **B774**, 127 (2007).

[18] H.-S. Lee, Phys. Lett. B **704**, 316 (2011).

[19] H. K. Dreiner, M. Hanussek, J.-S. Kim, and C. H. Kom, Phys. Rev. D **84**, 113005 (2011).

[20] S. Dimopoulos, R. Esmailzadeh, L. J. Hall, and G. D. Starkman, Phys. Rev. D **41**, 2099 (1990).

[21] G. Aad *et al.* (ATLAS Collaboration), Phys. Lett. B **708**, 37 (2012).

[22] S. Chatrchyan *et al.* (CMS Collaboration), Phys. Lett. B **704**, 123 (2011).

[23] ATLAS Collaboration, Report No. ATLAS-CONF-2011-126, 2011 (http://cdsweb.cern.ch/record/1383790). Recently, ATLAS published this analysis with a slightly modified event selection in [98].

[24] J. L. Hewett and T. G. Rizzo, in *Proceedings of the XXIX International Conference on High Energy Physics, Vancouver, 1998* (World Scientific, Singapore, 1999), Vol. II, p. 1698.

[25] H. K. Dreiner, P. Richardson, and M. H. Seymour, arXiv:hep-ph/9903419.

[26] H. K. Dreiner, P. Richardson, and M. H. Seymour, Phys. Rev. D **63**, 055008 (2001).

[27] H. K. Dreiner, P. Richardson, and M. H. Seymour, arXiv:hep-ph/0001224.

[28] P. Richardson, Ph.D. thesis, University of Oxford, 2000, arXiv:hep-ph/0101105.

[29] F. Deliot, G. Moreau, and C. Royon, Eur. Phys. J. C **19**, 155 (2001).

[30] H. K. Dreiner, S. Grab, M. Kramer, and M. K. Trenkel, Phys. Rev. D **75**, 035003 (2007).

[31] G. Moreau, M. Chemtob, F. Deliot, C. Royon, and E. Perez, Phys. Lett. B **475**, 184 (2000).

[32] G. Moreau, E. Perez, and G. Polesello, Nucl. Phys. **B604**, 3 (2001).

[33] R. J. Oakes, K. Whisnant, J. M. Yang, B.-L. Young, and X. Zhang, Phys. Rev. D **57**, 534 (1998).

[34] M. A. Bernhardt, H. K. Dreiner, S. Grab, and P. Richardson, Phys. Rev. D **78**, 015016 (2008).

[35] O. Cakir, S. Kuday, I. T. Cakir, and S. Sultansoy, Acta Phys. Pol. B **43**, 63 (2012).

[36] B. C. Allanach, M. Guchait, and K. Sridhar, Phys. Lett. B **586**, 373 (2004).

[37] H. K. Dreiner, S. Grab, and M. K. Trenkel, Phys. Rev. D **79**, 016002 (2009).

[38] C. Kilic and S. Thomas, Phys. Rev. D **84**, 055012 (2011).
[39] V. M. Abazov *et al.* (D0 Collaboration), Phys. Rev. Lett. **97**, 111801 (2006).
[40] C. T. Autermann, Report No. FERMILAB-THESIS-2006-46, 2006 (unpublished).
[41] V. M. Abazov *et al.* (D0 Collaboration), Phys. Rev. Lett. **100**, 241803 (2008); **105**, 191802 (2010).
[42] A. Abulencia *et al.* (CDF Collaboration), Phys. Rev. Lett. **96**, 211802 (2006).
[43] T. Aaltonen *et al.* (CDF Collaboration), Phys. Rev. Lett. **105**, 191801 (2010).
[44] A. Abulencia *et al.* (CDF Collaboration), Phys. Rev. Lett. **95**, 252001 (2005).
[45] D. Acosta *et al.* (CDF Collaboration), Phys. Rev. Lett. **95**, 131801 (2005).
[46] A. H. Chamseddine, R. L. Arnowitt, and P. Nath, Phys. Rev. Lett. **49**, 970 (1982).
[47] R. Barbieri, S. Ferrara, and C. A. Savoy, Phys. Lett. **119B**, 343 (1982).
[48] L. J. Hall, J. D. Lykken, and S. Weinberg, Phys. Rev. D **27**, 2359 (1983).
[49] G. L. Kane, C. F. Kolda, L. Roszkowski, and J. D. Wells, Phys. Rev. D **49**, 6173 (1994).
[50] A. Abulencia *et al.* (CDF Collaboration), Phys. Rev. Lett. **98**, 131804 (2007).
[51] V. M. Abazov *et al.* (D0 Collaboration), Phys. Lett. B **638**, 441 (2006).
[52] T. Aaltonen *et al.* (CDF Collaboration), Phys. Rev. Lett. **101**, 071802 (2008).
[53] S. Chakrabarti, M. Guchait, and N. K. Mondal, Phys. Lett. B **600**, 231 (2004).
[54] S. P. Das, A. Datta, and S. Poddar, Phys. Rev. D **73**, 075014 (2006).
[55] H. K. Dreiner, S. Grab, and T. Stefaniak, Phys. Rev. D **84**, 015005 (2011).
[56] J. Butterworth and H. K. Dreiner, Nucl. Phys. **B397**, 3 (1993); H. K. Dreiner and P. Morawitz, Nucl. Phys. **B503**, 55 (1997).
[57] T. Ahmed *et al.* (H1 Collaboration), Z. Phys. C **64**, 545 (1994); S. Aid *et al.* (H1 Collaboration), Z. Phys. C **71**, 211 (1996); A. Aktas *et al.* (H1 Collaboration), Eur. Phys. J. C **36**, 425 (2004).
[58] J. Breitweg *et al.* (ZEUS Collaboration), Eur. Phys. J. C **16**, 253 (2000); S. Chekanov *et al.* (ZEUS Collaboration), Phys. Rev. D **68**, 052004 (2003); Eur. Phys. J. C **50**, 269 (2007).
[59] ATLAS Collaboration, Eur. Phys. J. C **71**, 1809 (2011).
[60] G. Aad *et al.* (ATLAS Collaboration), Phys. Lett. B **707**, 478 (2012).
[61] S. Chatrchyan *et al.* (CMS Collaboration), Phys. Lett. B **704**, 411 (2011).
[62] S. Chatrchyan *et al.* (CMS Collaboration), Report No. CMS-PAS-EXO-11-045, 2011 [http://cdsweb.cern.ch/record/1393758/].
[63] G. Aad *et al.* (ATLAS Collaboration), Phys. Rev. D **85**, 012006 (2012).
[64] T. Banks, Y. Grossman, E. Nardi, and Y. Nir, Phys. Rev. D **52**, 5319 (1995).
[65] A. Heister *et al.* (ALEPH Collaboration), Eur. Phys. J. C **31**, 1 (2003).
[66] R. Barbier *et al.*, Phys. Rep. **420**, 1 (2005).
[67] G. Bhattacharyya, Nucl. Phys. B, Proc. Suppl. **52**, 83 (1997).
[68] B. C. Allanach, A. Dedes, and H. K. Dreiner, Phys. Rev. D **60**, 075014 (1999).
[69] Y. Kao and T. Takeuchi, arXiv:0910.4980.
[70] D. Choudhury, S. Majhi, and V. Ravindran, Nucl. Phys. **B660**, 343 (2003).
[71] L. L. Yang, C. S. Li, J. J. Liu, and Q. Li, Phys. Rev. D **72**, 074026 (2005).
[72] Y.-Q. Chen, T. Han, and Z.-G. Si, J. High Energy Phys. 05 (2007) 068.
[73] J. Pumplin, A. Belyaev, J. Huston, D. Stump, and W. K. Tung, J. High Energy Phys. 02 (2006) 032.
[74] A. D. Martin, R. G. Roberts, W. J. Stirling, and R. S. Thorne, Phys. Lett. B **531**, 216 (2002).
[75] A. D. Martin, R. G. Roberts, W. J. Stirling, and R. S. Thorne, Phys. Lett. B **604**, 61 (2004).
[76] S. Majhi, P. Mathews, and V. Ravindran, Nucl. Phys. **B850**, 287 (2011).
[77] L. Randall and R. Sundrum, Nucl. Phys. **B557**, 79 (1999).
[78] G. F. Giudice, M. A. Luty, H. Murayama, and R. Rattazzi, J. High Energy Phys. 12 (1998) 027.
[79] J. A. Bagger, T. Moroi, and E. Poppitz, J. High Energy Phys. 04 (2000) 009.
[80] H. Baer, S. de Alwis, K. Givens, S. Rajagopalan, and H. Summy, J. High Energy Phys. 05 (2010) 069.
[81] K. Choi and H. P. Nilles, J. High Energy Phys. 04 (2007) 006.
[82] H. E. Haber and G. L. Kane, Phys. Rep. **117**, 75 (1985).
[83] H. K. Dreiner, H. E. Haber, and S. P. Martin, Phys. Rep. **494**, 1 (2010).
[84] H. K. Dreiner and G. G. Ross, Nucl. Phys. **B365**, 597 (1991).
[85] M. A. Bernhardt, S. P. Das, H. K. Dreiner, and S. Grab, Phys. Rev. D **79**, 035003 (2009).
[86] H. K. Dreiner and S. Grab, Phys. Lett. B **679**, 45 (2009).
[87] K. Desch, S. Fleischmann, P. Wienemann, H. K. Dreiner, and S. Grab, Phys. Rev. D **83**, 015013 (2011).
[88] F. E. Paige, S. D. Protopopescu, H. Baer, and X. Tata, arXiv:hep-ph/0312045.
[89] P. Richardson, http://www.hep.phy.cam.ac.uk/richardn/HERWIG/ISAWIG/.
[90] G. Corcella, I. G. Knowles, G. Marchesini, S. Moretti, K. Odagiri, P. Richardson, M. H. Seymour, and B. R. Webber, J. High Energy Phys. 01 (2001) 010.
[91] G. Corcella *et al.*, arXiv:hep-ph/0210213.
[92] S. Moretti, K. Odagiri, P. Richardson, M. H. Seymour, and B. R. Webber, J. High Energy Phys. 04 (2002) 028.
[93] S. Ovyn, X. Rouby, and V. Lemaitre, arXiv:0903.2225.
[94] M. Cacciari, G. P. Salam, and G. Soyez, J. High Energy Phys. 04 (2008) 063.
[95] M. Cacciari and G. P. Salam, Phys. Lett. B **641**, 57 (2006).
[96] G. Aad *et al.* (ATLAS Collaboration), Phys. Rev. D **83**, 112006 (2011); Phys. Lett. B **709**, 158 (2012); **711**, 442(E) (2012).
[97] S. Chatrchyan *et al.* (CMS Collaboration), Phys. Lett. B **703**, 246 (2011); Report No. CMS-PAS-EXO-11-028, 2011, https://cdsweb.cern.ch/record/1405702.
[98] G. Aad *et al.* (ATLAS Collaboration), Phys. Rev. D **85**, 032004 (2012).